Hindawi
Advances in Civil Engineering
Volume 2021, Article ID 8822929, 17 pages
https://doi.org/10.1155/2021/8822929

Research Article

Research on Deformation Prediction of Foundation Pit Based on PSO-GM-BP Model

Dongge Cui,[1] **Chuanqu Zhu**,[1] **Qingfeng Li**,[2] **Qiyun Huang**,[1] **and Qi Luo**[1]

[1]*School of Resource & Environment and Safety Engineering, Hunan University of Science and Technology, Xiangtan, Hunan 411201, China*
[2]*Institute of Mineral Engineering, Hunan University of Science and Technology, Xiangtan, Hunan 411201, China*

Correspondence should be addressed to Dongge Cui; 170101040001@mail.hnust.edu.cn

Received 16 September 2020; Revised 2 November 2020; Accepted 28 December 2020; Published 16 January 2021

Academic Editor: Ali R. Vosoughi

Deformation prediction is significant to the safety of foundation pits. Against with low accuracy and limited applicability of a single model in forecasting, a PSO-GM-BP model was established, which used the PSO optimization algorithm to optimize and improve the GM (1, 1) model and the BP network model, respectively. Combining a small amount of measured data during the excavation of a bottomless foundation pit in a Changsha subway station, the calculations based on the PSO-GM model, the PSO-BP network model, and the PSO-GM-BP model compared. The results show that both the GM (1, 1) and BP neural network models can predict accurate results. The prediction optimized by the particle swarm algorithm is more accurate and has more substantial applicability. Due to its reliable accuracy and wide application range, the PSO-GM-BP model can effectively guide the construction of foundation pits, and it also has certain reference significance for other engineering applications.

1. Introduction

In-depth foundation pit engineering is a general term for a series of work carried out to ensure deep foundation pit construction safety and the surrounding environment not harmed. Safety construction and monitoring and early warning are also included [1]. Since the foundation pit's design cannot be entirely consistent with the actual situation, the construction conditions are complex and changeable. The environment of the foundation pit is also for various reasons. During the standard construction of the foundation pit, some uncontrollable conditions will also occur. When the deformation is severe, significant accidents such as the foundation pit's overall instability and the collapse of surrounding buildings may occur [2–4]. The purpose of foundation pit deformation monitoring is to ensure the smooth construction of foundation pit engineering so that the foundation pit deformation is within a safe and controllable range. Existing deformation evaluation indicators compare the amount of change and control value instead of using a more reasonable model to predict the foundation pit's deformation status to grasp the foundation pit's further development trend. So far, we have many mature deformation analysis methods. The more common ones are the regression method, time series analysis model, gray system analysis model, Kalman filter model, artificial neural network model, spectrum analysis method, etc. [5–10]. The application of machine learning methods in different engineering fields is becoming more and more extensive [11].

The deformation process of the foundation pit is an uncertain system with many factors and complicated construction conditions. Therefore, it could be regarded as a gray information system [12]. The GM (1, 1) model can extract the chaotic data series. Trends, generate new data columns and use them for predictive analysis [13]. Foundation pit deformation is a complex and nonlinear problem. The self-learning and self-adaptive ability of neural networks could be brought into full play. It has its unique advantages in the analysis of foundation pit deformation. BP network is a multilayer feedforward network used in deep foundation pit deformation prediction due to its error backpropagation

characteristics [14, 15]. Because of the deformation's complexity and the limitations of various forecasting models, it is a trend to forecast deformation accurately by using practical information of multiple models [16]. Due to some constraints of the prediction model itself, optimization algorithms or evolutionary algorithms are applied to engineering constructions [17–19].

The GM (1, 1) model and BP neural network were used for in-depth foundation pit prediction research because of their unique advantages. However, in actual application, it can be found that each model also has its shortcomings. This article will introduce a PSO algorithm to improve the two models and compare the prediction accuracy of the improved model and the original model.

2. PSO-GM (1, 1) Model

The establishment of the GM (1, 1) model firstly needs to accumulate the actual sequence once and generate the series$x^{(1)} = (x^{(1)}(1), x^{(1)}(2), \ldots, x^{(1)}(n))$, and use the generated string for analysis and prediction. The newly developed sequence of numbers increases regularly, and then an equation is established for prediction based on the increased regularity.

The time response of the GM (1, 1) model is as follows:

$$\hat{x}^{(1)}(k+1) = \frac{b}{a} + \left(x^{(0)}(1) - \frac{b}{a}\right)e^{-ak}. \quad (1)$$

It could be seen that the error of the GM (1, 1) model is firstly due to the selection of initial values, and the other is the estimation of gray parameters a and b. $\hat{u} = \begin{bmatrix} a & b \end{bmatrix}^T = (B^T B)^{-1} B^T Y$

The estimated costs of a and b depend on the construction method of the formula's background value$z^{(1)}(k)$.

Therefore, the GM (1, 1) model's prediction error mainly comes from the limited selection of the initial value and the background value construction formula's error. To reduce the error and improve the model's accuracy, the initial conditions separately and construct the background value was proposed to replace. Reselect the parameters used in the formula to optimize the GM (1, 1) model.

$x1(n)$ could $x^{(1)}(n)$be selected as GM (1, 1)$x^{(1)}(n)x^{(0)}(1)$'s initial condition so that the established model contains the best possible future predictions.

Then the time response sequence of GM (1, 1) is as follows:

$$\hat{x}^{(1)}(k+1) = \frac{b}{a} + \left(x^{(1)}(n) - \frac{b}{a}\right)e^{-a(k-n+1)}. \quad (2)$$

The simulated value is as follows:

$$\hat{x}^{(0)}(k+1) = \hat{x}^{(1)}(k+1) - \hat{x}^{(1)}(k) \quad k = 1, 2, \ldots, n. \quad (3)$$

When using the GM model for modeling, the construction formula of the background value is as follows:

$$z^{(1)}(k) = 0.5x^{(1)}(k) + 0.5x^{(1)}(k-1), \quad (4)$$

If the cumulative sequence slope is slow and the growth trend is not apparent, it is acceptable to use the trapezoidal area to replace the curve's shadow area on the interval. At this time, there is little difference between the two. Still, if the cumulative sequence slope is relatively high, if it is steep and the growth rate is speedy, the trapezoidal area formed is quite different from the interval curve's shadow area. Therefore, the background value construction formula is unreasonable at this time and contains specific errors, as shown in Figure 1.

The background value$z^{(1)}(k)$ is the critical area from the curve in the interval $[k-1, k]$ to the geometric sense's abscissa axis. The proper form of the background value that can satisfy unbiasedness is as follows:

$$z^{(1)}(k) = \int_{k-1}^{k} x^{(1)} \mathrm{d}t. \quad (5)$$

According to the integral median theorem, this is also equivalent to the linear combination of $x^{(1)}(k-1), x^{(1)}(k)$ and the parameter λ; that is, there is $\lambda \in [0,1]$ makes the following:

$$z^{(1)}(k) = \lambda x^{(1)}(k-1) + (1-\lambda)x^{(1)}(k). \quad (6)$$

The value of the parameter λ will have a direct impact on the model prediction accuracy. At this time, we have a model parameter optimization problem, combined with the characteristics of the particle swarm algorithm that is good at global optimization, so that complicated formula derivation was avoided, and the thinking is clear and easy to implement.

The following is the process of the PSO algorithm to find the optimal λ:

Step 1: Initialize the population. Randomly generate a sequence on the interval [0, 1]:$\lambda = (\lambda_1, \lambda_2, \ldots, \lambda_n)$, each of λ represents the possible weight of the randomly generated background value.

Step 2: Calculate fitness. The fitness function should choose the mean square error function SSE, replace all the generated λ_i to calculate the background value, construct a new background value formula, and use it in the GM (1, 1) model for prediction and the predicted value. The average value of the absolute value of the relative error of the true value is used as the fitness value of the corresponding individual.

Step 3: Compare the current fitness value of the particle with the optimal historical value. If it is better than the optimal historical value, replace its current position with the best position of the particle; compare the current fitness value of the particle with the optimal group value, if it is excellent. If it is at the optimal value of the group, its current position will replace the best position of the group.

Step 4: Update the particles according to the following formula:

$$v_{id}^{k+1} = \omega \cdot v_{id}^{k} + c_1 \cdot \text{rand}(\,) \cdot \left(p_{id}^{k} - x_{id}^{k}\right) + c_2 \cdot \text{rand}(\,) \cdot \left(p_{gd}^{k} - x_{id}^{k}\right), \quad (7)$$
$$x_{id}^{k+1} = x_{id}^{k} + v_{id}^{k+1},$$

In the formula, $c1$ and $c2$ called learning factors or acceleration factors; rand() is a random number between (0, 1); v_{id}^{k} and x_{id}^{k} are the velocity of the particle i in the dth dimension in the kth iteration, respectively, And position p_{id}^{k} is the position of the extreme individual value of the particle i in the dth dimension; p_{gd}^{k} is the position of the extreme global value of the group in the dth dimension.

Step 5: If the fitness value is not sufficiently good or the preset maximum number of iterations was not obtained, return to step (2).

Through the above steps, the optimal λ_i was found through iteration, and then the optimal background value construction formula is calculated, and then the next step is predicted, as shown in Figure 2.

3. Determination of PSO-BP Network

The combination of BP network and PSO algorithm uses the global search and local search capabilities of both giving full play to their respective advantages, preventing the network from overfitting and falling into local extremums, and at the same time obtaining a faster convergence speed. Randomly initialize the position of the particles in the PSO algorithm. The position of each particle corresponds to a set of weights and thresholds in the BP network. The PSO algorithm was used to iteratively train the network until the optimal particle position is output, the optimal weight, and the threshold. Finally, use this optimized network for prediction. When simulating actual data, to minimize the neural network's average relative error, its fitness function is as follows:

$$E = \frac{1}{m} \sum_{j=1}^{m} \left(d_j - y_j\right)^2. \quad (8)$$

The specific steps of the PSO-BP algorithm were described as follows (see Figure 3):

(1) Initialization. Set the relevant parameters of the PSO-BP network. Determine network structure, including the number of layers of the system and the number of neurons in each layer. Determine the particle group related parameters, including the initial inertia weight w, the learning factors c1 and c2, the maximum number of iterations T, and the number of swarm N. When determining the number of populations, the dimension D of the particles to be optimized should be considered the total number of weight thresholds. The total number of weight thresholds that the PSO algorithm needs to optimize is the following:

$$D = (l+1)^{*} n + (n+1)^{*} m, \quad (9)$$

l is the number of input neurons; n is the number of hidden layer neurons; m is the number of neurons in the output layer. Finally, the particle's velocity and position were randomly initialized.

(2) Calculating the fitness value of each particle according to the fitness function selected by the problem. The fitness function is as follows:

$$E = \frac{1}{m} \sum_{j=1}^{m} \left(d_j - y_j\right)^2. \quad (10)$$

(3) Compare the current fitness value and the optimal historical value of the particle. If it is better than the optimal historical value, replace its current position with the particle's best position; compare its current fitness value with the optimal amount of the group. For the group's optimal cost, replace its current situation with the best part of the group.

(4) Iterative evolution of the velocity and position of the particle according to the speed and position update formula.

$$v_{id}^{k+1} = \omega \cdot v_{id}^{k} + c_1 \cdot \text{rand}(\,) \cdot \left(p_{id}^{k} - x_{id}^{k}\right) + c_2 \cdot \text{rand}(\,) \cdot \left(p_{gd}^{k} - x_{id}^{k}\right), \quad (11)$$
$$x_{id}^{k+1} = x_{id}^{k} + v_{id}^{k+1}.$$

(5) If the excellent fitness value or the preset maximum iteration number was not reached, then return to step (2). If the condition was met, the global optimal particle position of the output is the optimal BP network weight and threshold.

(6) After the weight threshold is output, the neural network training continued until the result is output.

4. PSO-GM-BP Model Combination Forecast

The foundation pit's deformation process is usually a nonstationary process, which usually presents trend and randomness characteristics. Therefore, the deformation monitoring data could be decomposed into trend items and random items. It is an effective method to use a suitable prediction model to predict each decomposition item accurately (see Figure 4).

The gray forecast model is good at extracting the trend item information contained in the deformation information. It has its unique advantages for forecasting trend items by accumulating and generating new data columns to enhance the trend characteristics. Foundation pit deformation is a complex and nonlinear problem, and the self-learning and self-adaptive capabilities of the BP neural network could be used well. The randomness of deformation could be extracted with high precision. The combined prediction of GM (1, 1) and BP network had been widely used in foundation pit monitoring, but the two models participating in

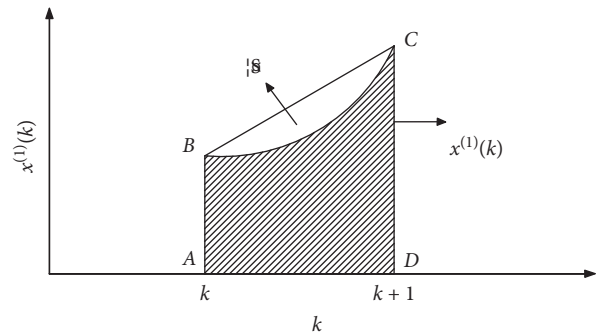

Figure 1: Error generating mechanism of background value.

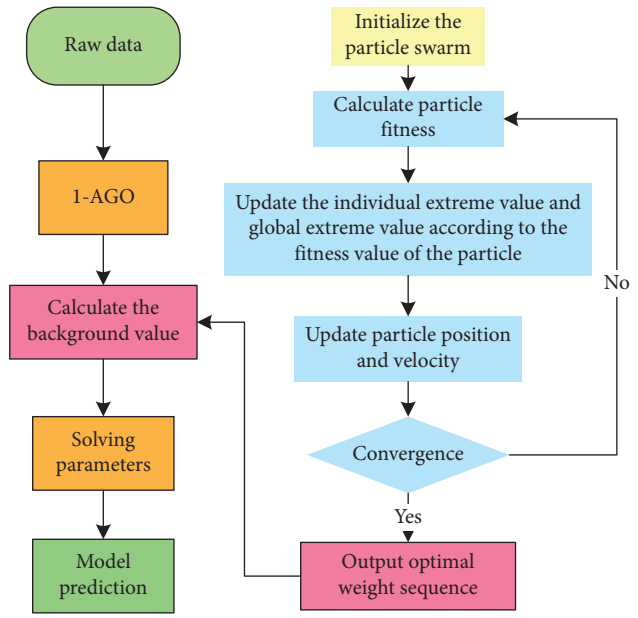

Figure 2: Flow chart of particle swarm optimization GM (1, 1) model.

combined forecasts were connected with their shortcomings. They also bring about some errors that could have been avoided. This paper adopts the optimized PSO-BP network and PSO-GM (1, 1) model combination prediction under the premise of small samples, comprehensively considering the advantages of high precision and less information and analyzing the foundation's deformation data pits. Make accurate predictions to guide the safe construction of foundation pits.

The modeling steps of combined forecasting are as follows (see Figure 5):

(1) Use the PSO-GM (1, 1) model to fit and predict the original data, extract the trend items contained therein, and obtain the predicted value and the corresponding residual sequence:

$$\hat{x}^{(0)}(k) = \left\{\hat{x}^{(0)}(1), \hat{x}^{(0)}(2), \ldots, \hat{x}^{(0)}(n)\right\}, \tag{12}$$

$$e(k) = x^{(0)}(k) - \hat{x}^{(0)}(k) = \{e(1), e(2), \ldots, e(n)\}. \tag{13}$$

(2) Use the residual sequence to train the PSO-BP network and obtain the residual after the second correction:

$$\hat{e}(k) = \{\hat{e}(1), \hat{e}(2), \ldots, \hat{e}(n)\}. \tag{14}$$

(3) Finally, add the predicted value of the PSO-GM (1, 1) model and the corrected residual to get the final predicted value:

$$\hat{x}(k) = \hat{x}^{(0)}(k) + \hat{e}(k). \tag{15}$$

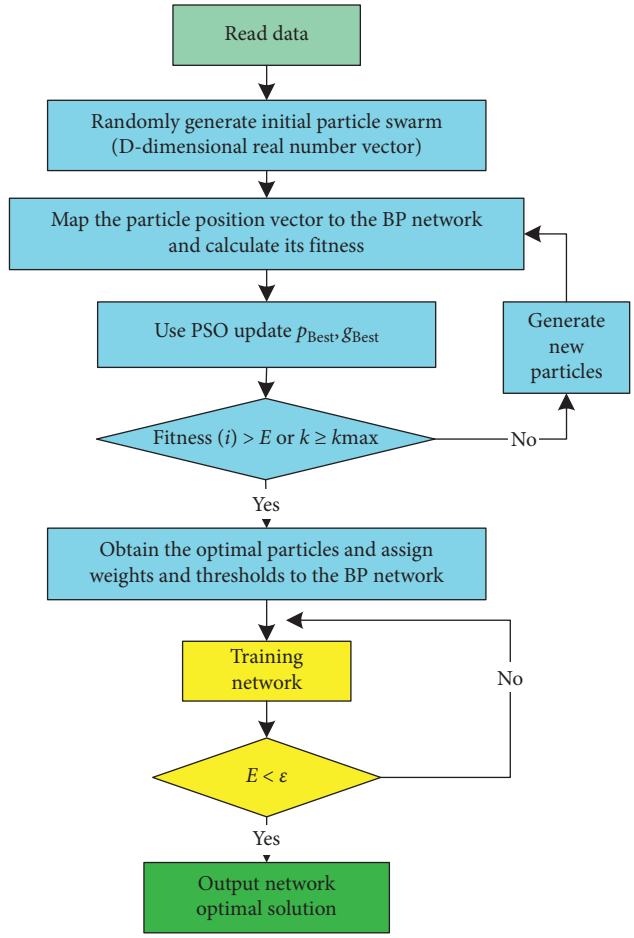

Figure 3: PSO- BP network flow chart.

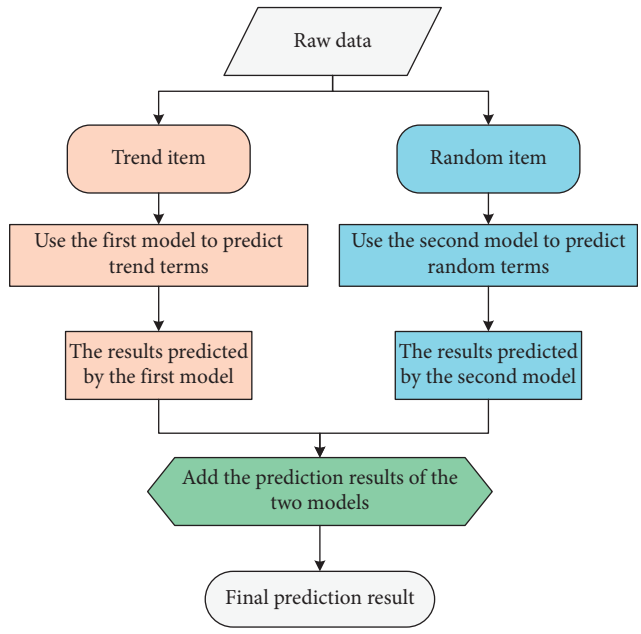

Figure 4: Combined forecasting flow chart.

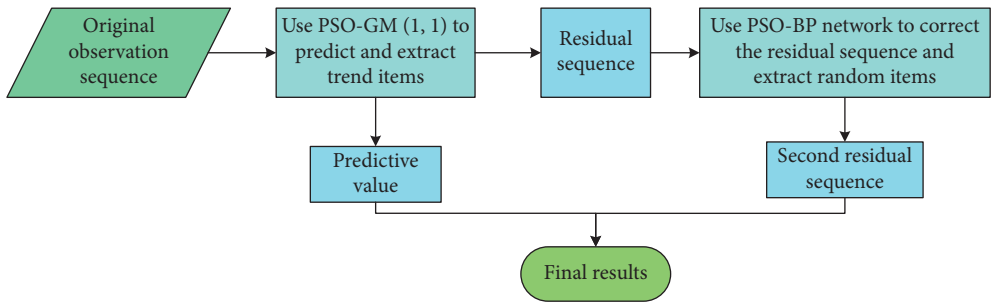

Figure 5: PSO-GM (1, 1) and PSO-BP network combination forecasting.

5. Engineering Application Example

5.1. Project Overview. Yingwanzhen Station is the tenth station of the first phase of Changsha Metro Line 4 (Purui Avenue ~ Guihua Avenue), and it also is the interchange station of Line 2 and Line 4. The mileage of the significant platform center of Yingwanzhen Station is DK27 + 192.000, and the platform width is about 14 m. The station is located in the Greenland Group's development zone on the north side of Fenglin 1 road and Lushan Road and passes through Yingwan Road, which was arranged in a north-south direction. Yingwanzhen Station is an island platform station with four underground floors (partial three feet). The total length of outsourced stations is 272.7 m, and the standard section width is 23.3 m. The main body of Yingwanzhen Station was constructed by the open-cut method. The foundation pit's depth is 28.14 m during construction, and the depth of the support structure is up to 36.58 m. The station's enclosure structure to the south of the 13th axis adopts a 1000 mm underground continuous wall with a standard section width of 6 m; the north area adopts the grading excavation + drilling pile support method, with a pile diameter of 1200 mm and a pile spacing of 1350 mm. A row of 34 vertical columns was set along the foundation pit's centerline, which reduces the span and improves the support's bending performance. Two rows of uplift piles were set along the foundation pit's two sides of the centerline. The mounds have a diameter of 1500 m and a total of 66 stacks. The depth can reach 50 m. The shield shaft at the north end of the station uses two concrete supports, and the beam at the south end uses five substantial supports; the standard section uses seven supports for the −25 axis and four supports for the 26 axes to the 34 axes. The first and third supports of the station are concrete supports, and the second, fourth, and fifth supports are steel supports. Both ends of the station are shield starting wells, with four securities starting one after another. The project is large, and the construction period is tight. It is a control site on the whole line.

5.2. Data Selection. Priority should be given to the analysis of the high-risk supporting force and inclinometer data. The subsequent deformation trend could be effectively used to ensure the safety of the foundation pit. The actual measurement data at 15 m (after this referred to as B16) of the support force monitoring point ZL2-7 in the regular monitoring period and the wall inclinometer monitoring point B16 during the alarm period were selected for analysis and verification. The monitoring data of ZL2-7 and B16 are as follows, as shown in Tables 1 and 2.

As shown in Table 2, the B16 data is more significant than 30 mm from the 11th-period information, which belongs to the data exceeding the alarm value in the deformation monitoring work and belongs to the orange warning category. How to carry out the next construction while ensuring that the monitoring data does not continue to increase is a big problem. It is a more significant challenge for the safety of the entire foundation pit. Therefore, accurate prediction of the data at this point becomes particularly important.

5.3. Support Force Prediction and Analysis

5.3.1. PSO-GM (1, 1) Model Prediction. The GM (1, 1) model and the optimized PSO-GM (1, 1) model were used to model and analyze the measured data. The data used is the 15-period data of ZL2-7 monitoring points. Two models are used to fit and analyze the first 12-period data to predict the 13th to 15th periods' deformation and finally evaluate the two models' accuracy.

The calculation results based on GM (1, 1) model and the PSO-GM (1, 1) model are shown in Table 3, and the accuracy evaluation results are shown in Table 4. The prediction results are based on the original grey model and based on the PSO-GM (1, 1) model shown in Table 5.

The posterior difference ratios based on the original gray model and based on the PSO-GM (1, 1) model are 0.1424 and 0.1269. The small error probability of the two models is both 1. The original gray model's accuracy evaluation results and the PSO-GM (1, 1) model meet the prediction model's excellent standards. Still, the variance based on the PSO-GM (1, 1) model is smaller, indicating that its prediction accuracy is better. It can be seen from Table 5 that for the prediction results, the relative errors of the GM (1, 1) model are 2.67%, 8.31%, and 8.59%, respectively, while the relative errors of the PSO-GM (1, 1) model are 1.69 %, 5.73%, 5.06%. The prediction accuracy based on the PSO-GM (1, 1) model is higher, and the model and prediction results are more stable (see Figure 6). The relative errors and posterior difference ratios were significantly reduced, indicating that the

Table 1: ZL2-7 monitoring value.

Period	Monitoring value (kN)
1	1091.74
2	1227.01
3	1343.88
4	1578.08
5	1757.89
6	1822.97
7	1828.44
8	1908.81
9	2061.54
10	2025.6
11	2151.51
12	2221.34
13	2350.88
14	2342.03
15	2455.03

Table 2: Cumulative value of B16 monitoring points.

Period	Cumulative value (mm)
1	21.66
2	23.30
3	23.90
4	23.25
5	24.50
6	25.31
7	27.95
8	29.04
9	28.23
10	29.44
11	30.38
12	30.81
13	31.23
14	31.92
15	32.44

accuracy and stability of the model have been greatly improved. The results show that the PSO algorithm is effective and stable for the optimization of the GM (1, 1) model.

5.3.2. PSO-BP Model Prediction. The BP network and the PSO-BP network were used to predict and analyze the monitoring data. The data used is the 15th phase of the ZL2-7 monitoring point. The monitoring data of degrees 1–12 were used as training samples, and the data of the latter three stages are test samples.

To avoid numerical problems and improve network convergence, normalize the sample data before training. The input neuron was set to 5, and the output neuron was 1. The period 1–5 was used as the input, and the data of period six was used as the output. After normalization, the result is output. The number of hidden layer neurons tested to find that the prediction effect is the best when the number of nodes is 6.

The following are the training effect diagrams of the BP network and the PSO-BP system (see Figures 7 and 8):

The target error is achieved in the BP network training diagram when the network training reaches 142 times. In the PSO-BP network training diagram, the network converges quickly because of the particle swarm algorithm's optimal initial weights and thresholds. The training goal was reached at the 68th training. It shows that the convergence of the BP network optimized by PSO was strengthened.

When using the two systems for prediction, the training effect is very close (see Figures 9 and 10). Still, in terms of generalization ability, as shown in Figures 11 and 12, the PSO-BP system has significantly improved compared to the BP network. The comparison of the overall data is as follows (see Tables 6 and 7, and Figure 13). As shown in Tables 6 and 7, the relative errors of the BP network are 5.21%, 3.07%, and 4.47%, respectively, while the relative errors of the PSO- BP network are 1.95 %, 2.00%, and 2.01%. The relative errors were significantly reduced, indicating that the accuracy and stability of the model have been greatly improved. The results show that the PSO algorithm is effective and stable for the optimization of the BP network.

5.3.3. PSO-GM-BP Model Combination Forecast. It could be seen from Table 6 that the monitoring value of ZL2-7 has an apparent increasing trend, and there is also large volatility. Therefore, the ZL2-7 monitoring value can be decomposed into trend items and random items to establish a combined forecasting model in the integrated forecasting. The data used is the 15-period data of the ZL2-7 monitoring point. The PSO-GM (1, 1) model is used to fit and analyze the first 12 periods' data, and the trend item was predicted for the 13–15 periods. The PSO-BP network is used for residual error correction random item prediction (see Figures 14 and 15).

As shown in Tables 8 and 9, the relative errors of the PSO-GM (1, 1) model were 1.69%, 5.73%, and 5.06%, and the relative errors of the PSO-BP network were 1.95%, 2.00%, and 2.01%, respectively, while the relative errors of the PSO-BP network were 1.45%,0.60%, and 1.94%. The average relative errors of the three models were 4.16%,1.98%, and 1.33%. The accuracy of the three models is sorted from high to low as follows: PSO-GM-BP model, PSO-BP network, and PSO-GM (1, 1) model. With the optimization of the PSO algorithm, the accuracy, efficiency, and stability of the GM (1, 1) model and BP network have been improved. The PSO-GM-BP model has the best prediction effect and can provide effective and efficient data support for foundation pit construction.

5.4. Inclination Data Prediction and Analysis

5.4.1. PSO-GM (1, 1) Model Prediction. The original GM (1, 1) model and the optimized PSO-GM (1, 1) model were used to model and analyze the measured data. The data used is the 15-period data of the B16 monitoring point. The calculation results were shown in Table 10, and the accuracy evaluation results shown in Table 11.

Through the calculation results in Table 11, it could be found that the posterior difference ratios based on the original gray model and the PSO-GM (1, 1) model are 0.1508 and 0.1072, respectively, and the small error probability of

Table 3: Actual value and model fitting value of ZL2-7.

Period	Actual value	GM (1, 1)		PSO-GM (1, 1)	
		Fitting value	Relative error (%)	Fitting value	Relative error (%)
1	1091.74	1091.74	0	1022.855	−6.30
2	1227.01	1396.89	−13.85	1397.199	−13.82
3	1343.88	1468.10	−9.24	1469.021	−9.31
4	1578.08	1542.94	−2.23	1544.535	−2.12
5	1757.89	1621.59	−7.75	1623.931	−7.62
6	1822.97	1704.25	−6.51	1707.408	−6.33
7	1828.44	1791.12	−2.04	1795.176	−1.81
8	1908.81	1882.42	−1.38	1887.456	−1.11
9	2061.54	1978.38	−4.03	1984.479	−3.73
10	2025.6	2079.23	−2.65	2086.49	−3.00
11	2151.51	2185.22	−1.57	2193.745	−1.96
12	2221.34	2296.61	−3.39	2306.513	−3.83

Table 4: Accuracy assessment table.

Model	C	*P*
GM (1, 1)	0.1424	1
PSO-GM (1, 1)	0.1269	1

Table 5: Comparison of actual and predicted values of ZL2-7.

Period		13	14	15
Actual value		2350.88	2342.03	2455.03
GM (1, 1)	Predicted value	2413.68	2536.72	2666.03
	Relative error (%)	−2.67	−8.31	−8.59
PSO-GM (1, 1)	Predicted value	2390.73	2476.32	2579.31
	Relative error (%)	−1.69	−5.73	−5.06

the two models is both 1. The original gray model's accuracy evaluation results and the PSO-GM (1, 1) model meet the prediction model's excellent standards. Still, the variance based on the PSO-GM (1, 1) model is smaller, indicating that its prediction accuracy is better. It can be seen from Table 5 that for the prediction results, the relative errors of the GM (1, 1) model were 3.55%, 3.37%, and 3.62%, respectively, while the relative errors of the PSO-GM (1, 1) model were 2.18 %, 1.98%, and 2.30%. The prediction accuracy based on the PSO-GM (1, 1) model is higher, and the model and prediction results are more stable (see Figure 16). The relative errors and posterior difference ratios were significantly reduced, indicating that the accuracy and stability of the model have been greatly improved. The results show that the PSO algorithm is effective and stable for the optimization of the GM (1, 1) model.

5.4.2. PSO-BP Model Prediction. The BP network and the PSO-BP network were used to predict and analyze the monitoring data. The data used is the 15th phase of the B16 monitoring point. The monitoring data of degrees 1–12 were used as training samples, and the data of the latter three stages are test samples.

To avoid numerical problems and improve network convergence, normalize the sample data before training. After normalization, the result is output. The number of hidden layer neurons was tested repeatedly to find that when the number of nodes is 7, the prediction effect is the best.

The following are the training effect diagrams of the BP network and the PSO-BP system:

In the BP network training diagram, the target error was achieved when the network training reaches 200 times; in the PSO-BP network training diagram, the network performance was degraded because of the particle swarm algorithm's optimal initial weight and threshold. The training goal was reached on the 128th training session. It shows that the convergence of the BP network optimized by PSO was strengthened (see Figures 17 and 18).

When using two networks for prediction, the training data is not much different (see Figures 19 and 20). Still, in terms of generalization ability, as shown in Figures 21 and 22, the PSO-BP system significantly improves the BP network. The comparison of the overall data is as follows (see Tables 12 and 13 and Figure 23). As shown in Tables 12 and 13, the relative errors of the BP network were 9.54%, 6.21%, and 3.93%, respectively, while the relative errors of the PSO-BP network were 0.11%, 0.96%, and 0.82%. The relative errors were significantly reduced, indicating that the accuracy and stability of the model have been greatly improved. The results show that the PSO algorithm is effective and stable for the optimization of the BP network.

5.4.3. PSO-GM-BP Model Combination Forecast. It could be seen that the B16 monitoring value also has an obvious increasing trend and considerable volatility. Therefore, in combined forecasting, the B16 monitoring value can be decomposed into trend items and random items to establish a combined forecasting model. The data used is the 15-period data of the B16 monitoring point. The PSO-GM (1, 1) model is used to fit and analyze the first 12-period data, the trend item was predicted for the 13–15 period, and the PSO-BP network is used for residual. Correct the random thing forecast (see Figures 24 and 25).

As shown in Tables 14 and 15, the relative errors of the PSO-GM (1, 1) model were 2.18%, 1.98%, and 2.30%, and the relative errors of the PSO-BP network were 0.11%, 0.96%, and 0.82%, respectively, while the relative errors of the PSO-BP network were 0.20%, 0.10%, and 0.20%. The average

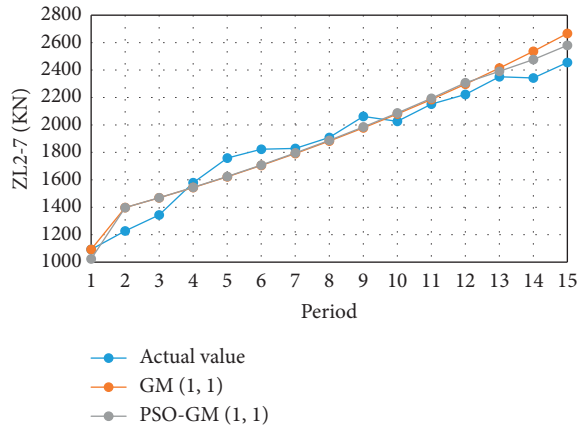

Figure 6: Comparison of actual and predicted values.

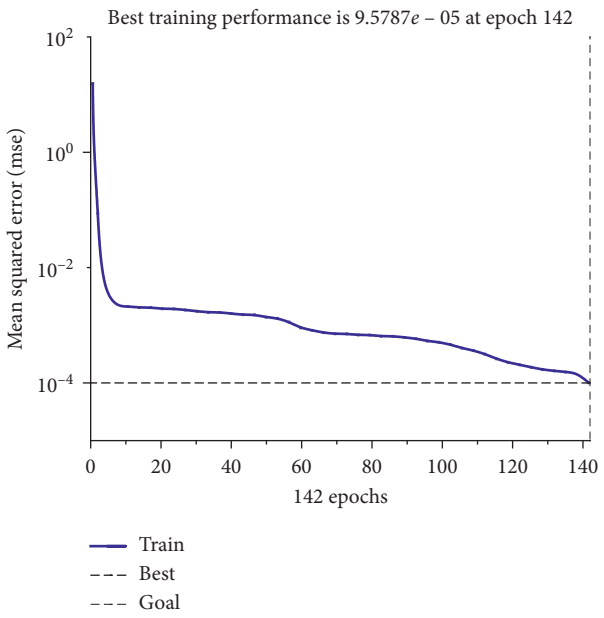

Figure 7: BP network training diagram.

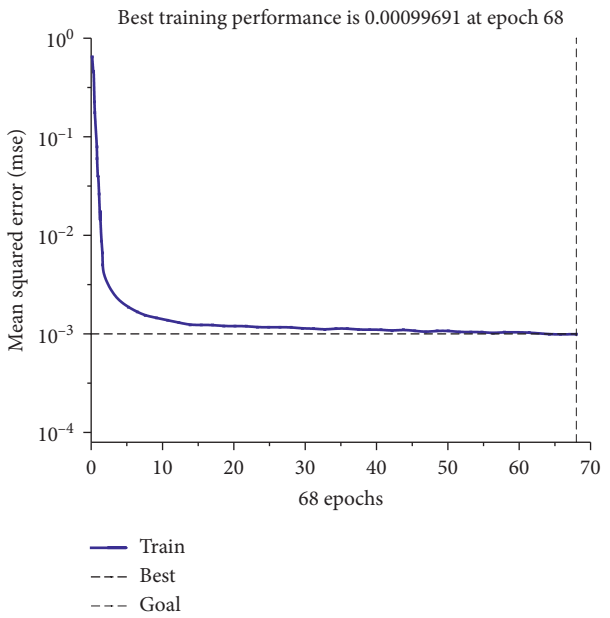

Figure 8: PSO-BP network training diagram.

relative errors of the three models were 2.15%, 0.63%, and 0.17%. The accuracy of the three models are sorted from high to low as follows: PSO-GM-BP model, PSO-BP network, PSO-GM (1, 1) model. With the optimization of the PSO algorithm, the accuracy, efficiency, and stability of the GM (1, 1) model and BP network have been improved. The PSO-GM-BP model has the best prediction effect and can provide effective and efficient data support for foundation pit construction.

6. Results and Discussion

(1) The average relative errors of the three models for support force prediction were 4.16%, 1.98%, and 1.33%, and the average relative errors of the three models for support force prediction were 2.15%, 0.63%, and 0.17%.

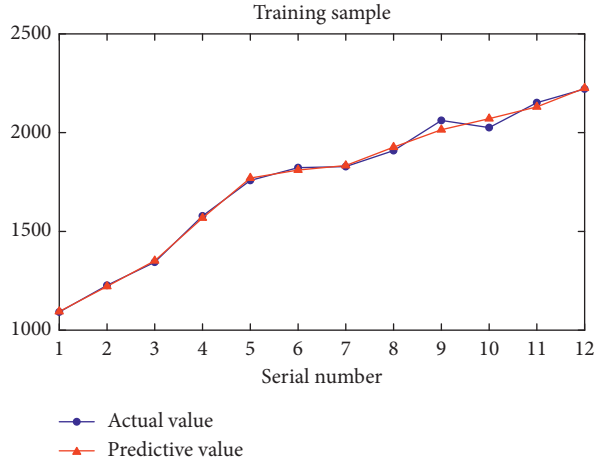

Figure 9: BP network training sample.

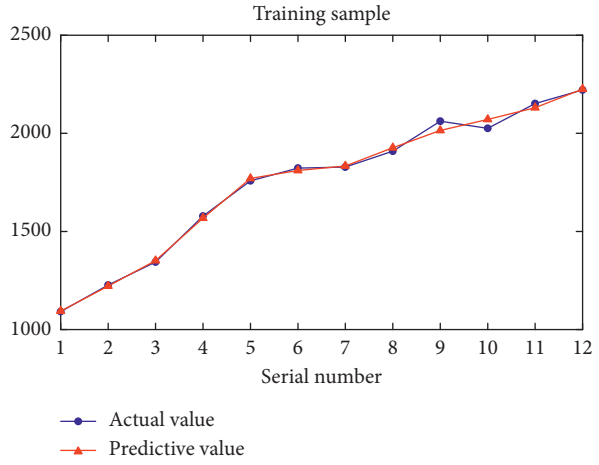

Figure 10: PSO-BP network training sample.

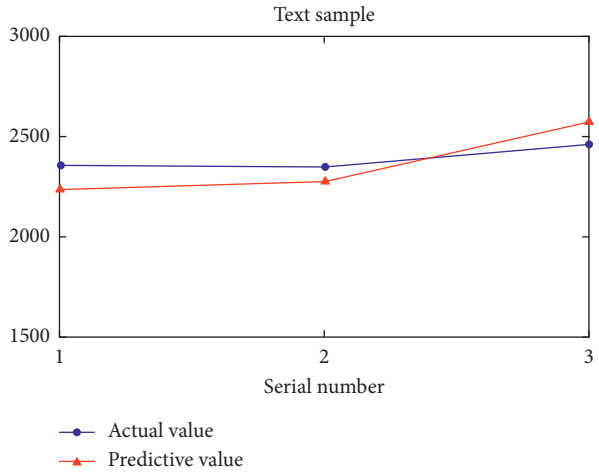

Figure 11: BP network test sample.

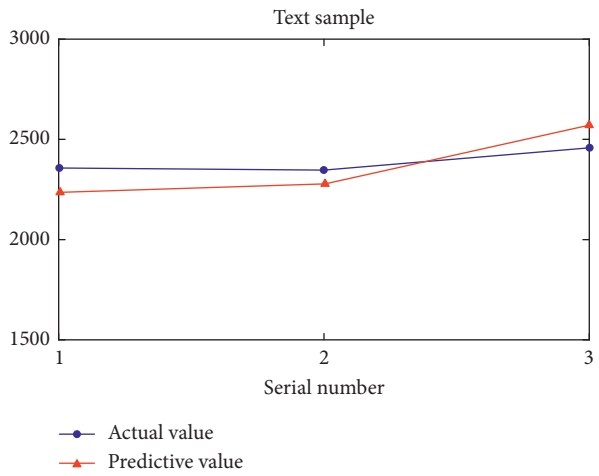

Figure 12: PSO-BP network test sample.

(2) Analyze the error source of the GM (1, 1) model, apply the global optimization feature of the PSO algorithm to optimize the parameters of the background value construction formula of the GM (1, 1) model, and propose an optimized PSO-GM (1, 1) Model. Combining axial force and inclinometer

Table 6: ZL2-7 actual value and model fitting value.

Period	Actual value	BP network		PSO-BP network	
		Fitting value	Relative error (%)	Fitting value	Relative error (%)
1	1091.74	1094.02	−0.21	1096.139	−0.40
2	1227.01	1221.387	0.46	1226.61	0.03
3	1343.88	1351.156	−0.54	1345.639	−0.13
4	1578.08	1567.732	0.65	1576.096	0.12
5	1757.89	1770.027	−0.69	1760.421	−0.14
6	1822.97	1810.918	0.66	1821.395	0.08
7	1828.44	1833.811	−0.29	1828.591	−0.01
8	1908.81	1926.841	−0.94	1908.798	0
9	2061.54	2014.674	2.27	2061.533	0
10	2025.6	2070.983	−2.24	2025.602	0
11	2151.51	2130.434	0.98	2151.51	0
12	2221.34	2225.197	−0.17	2221.34	0

Table 7: ZL2-7 actual value and predicted value comparison results table.

Period		13	14	15
Actual value		2350.88	2342.03	2455.03
BP network	Predicted value	2228.461	2270.236	2564.764
	Relative error (%)	5.21	3.07	−4.47
PSO-BP network	Predicted value	2305.01	2388.83	2405.64
	Relative error (%)	1.95	−2.00	2.01

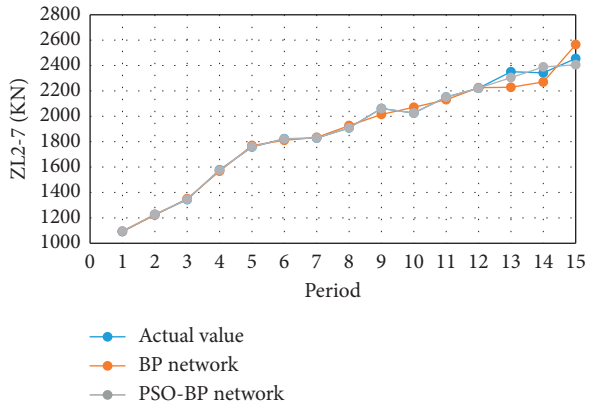

Figure 13: Comparison of actual and predicted values.

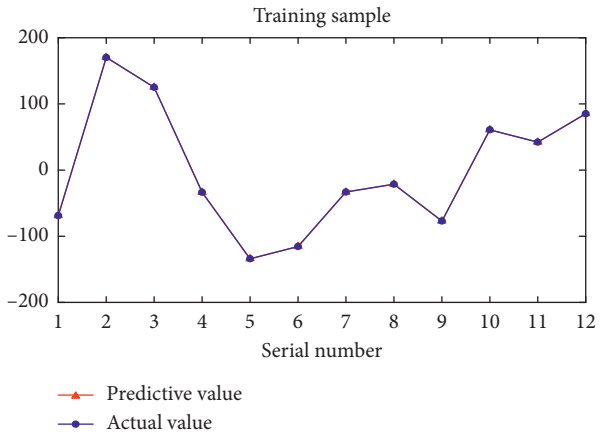

Figure 14: Residual training samples.

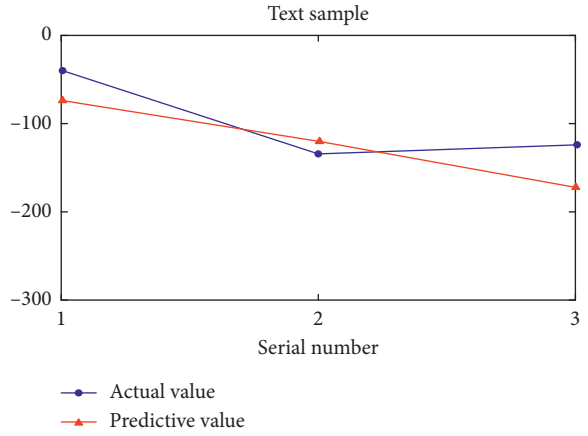

Figure 15: Residual test samples.

Table 8: Comparison of three models.

Period	Actual value	Predicted value		
		PSO-GM (1, 1)	PSO-BP	PSO-GM-BP
13	2350.88	2390.73	2305.01	2316.65
14	2342.03	2476.32	2388.83	2356.05
15	2455.03	2579.31	2405.64	2407.19

Table 9: Comparison of relative error of three models.

Period	Relative error (%)		
	PSO-GM (1, 1)	PSO-BP	PSO-GM-BP
13	−1.69	1.95	1.45
14	−5.73	−2	−0.60
15	−5.06	2.01	1.94
Average relative error	4.16	1.98	1.33

Table 10: Actual and simulated results of B16.

Period	Actual value	GM (1, 1)		PSO-GM (1, 1)	
		Fitting value	Relative error (%)	Fitting value	Relative error (%)
1	21.66	21.6600	0.00	21.1069	2.55
2	23.30	22.8930	1.75	22.6821	2.65
3	23.90	23.6234	1.16	23.4549	1.86
4	23.25	24.3771	4.85	24.2521	4.32
5	24.50	25.1548	2.67	25.0804	2.37
6	25.31	25.9574	2.56	25.9350	2.47
7	27.95	26.7856	4.17	26.8186	4.05
8	29.04	27.6402	4.82	27.7323	4.50
9	28.23	28.5220	1.03	28.6772	1.58
10	29.44	29.4320	0.03	29.6543	0.73
11	30.38	30.3711	0.03	30.6646	0.94
12	30.81	31.3400	1.72	31.7094	2.92
13	31.23	32.3399	3.55	31.9099	2.18
14	31.92	32.9946	3.37	32.5515	1.98
15	32.44	33.6142	3.62	33.1876	2.3

Table 11: Accuracy assessment table.

Model	C	P
GM (1, 1)	0.1508	1
PSO-GM (1, 1)	0.1072	1

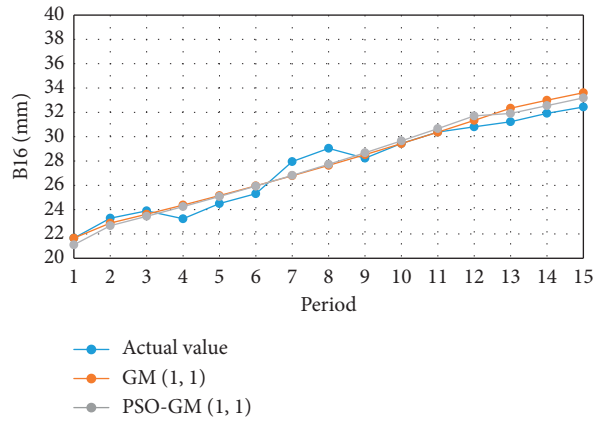

Figure 16: Comparison of actual and predicted values.

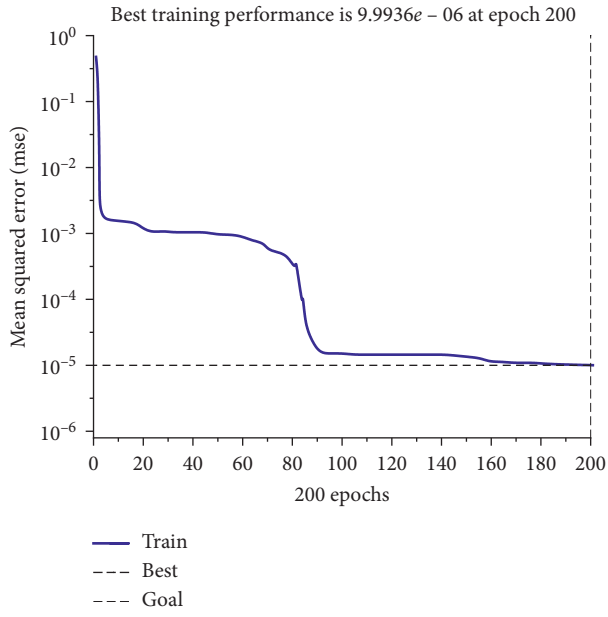

Figure 17: BP network training diagram.

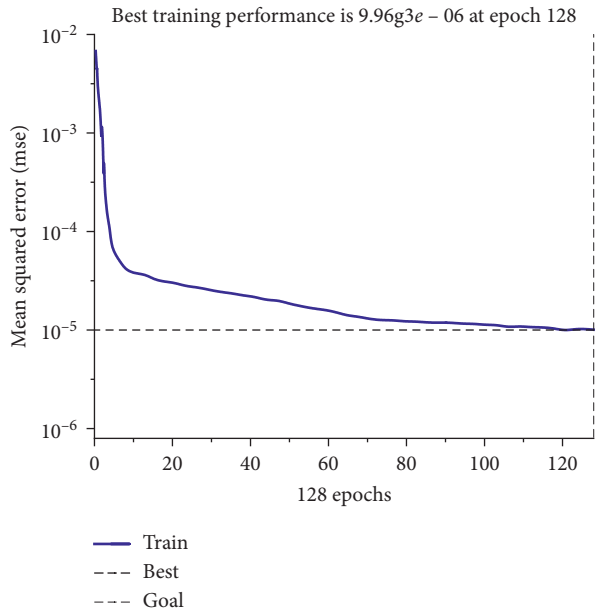

Figure 18: PSO-BP network training diagram.

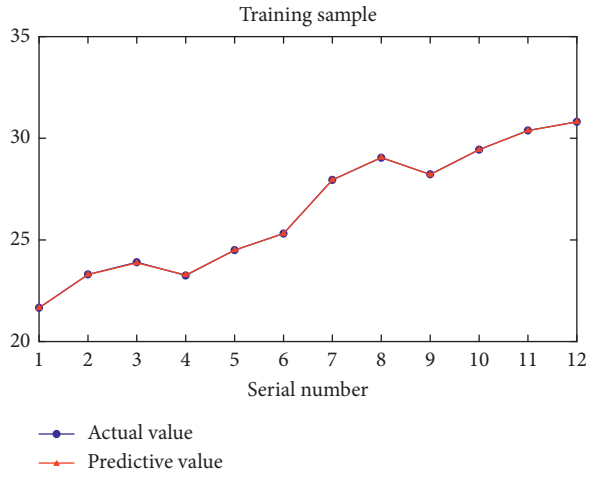

Figure 19: BP network training sample.

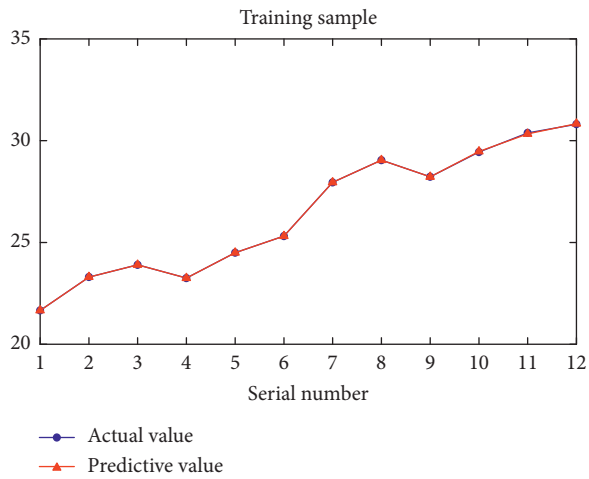

Figure 20: PSO-BP network training sample.

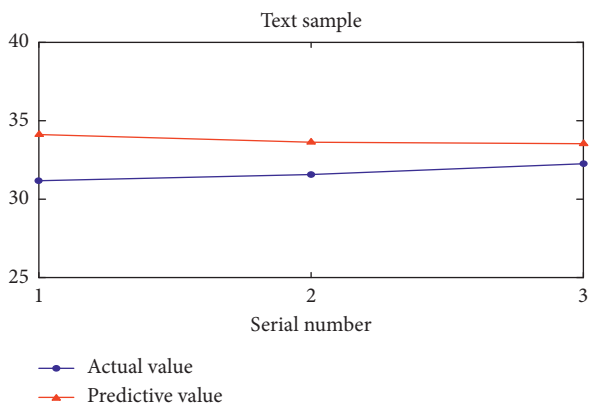

Figure 21: BP network test sample.

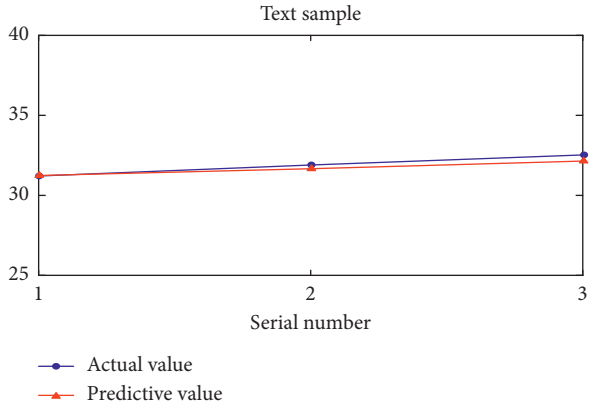

Figure 22: PSO-BP network test sample.

Table 12: B16 actual value and model fitting value results.

Period	Actual value	BP network		PSO-BP network	
		Fitting value	Relative error (%)	Fitting value	Relative error (%)
1	21.66	21.6528	−0.03	21.6594	0.00
2	23.30	23.2941	−0.02	23.2997	0.00
3	23.90	23.8606	−0.16	23.8993	0.00
4	23.25	23.2772	0.12	23.2501	0.00
5	24.50	24.4945	−0.02	24.4982	−0.01
6	25.31	25.3054	−0.02	25.3095	0.00
7	27.95	27.9457	−0.01	27.9483	−0.01
8	29.04	29.0528	0.04	29.0400	0.00
9	28.23	28.2108	−0.07	28.2220	−0.03
10	29.44	29.4375	−0.01	29.4683	0.10
11	30.38	30.3777	−0.01	30.3346	−0.15
12	30.81	30.8088	−0.00	30.8323	0.07

Table 13: B16 actual value and predicted value comparison results.

Period		13	14	15
BP network	Actual value	31.23	31.92	32.44
	Predicted value	34.2091	33.9029	33.7154
	Relative error (%)	9.54	6.21	3.93
PSO-BP network	Predicted value	31.1965	31.6132	32.1754
	Relative error (%)	−0.11	−0.96	−0.82

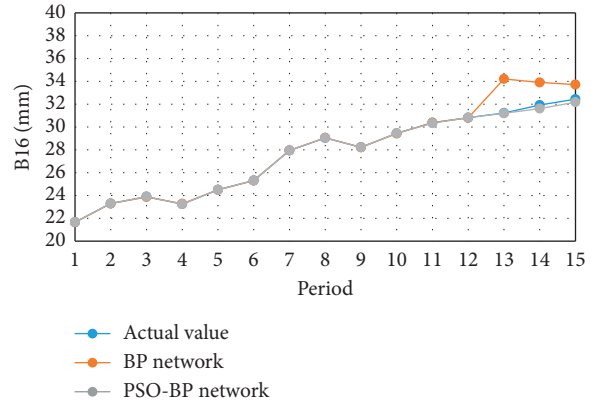

Figure 23: Comparison of the actual and predicted value.

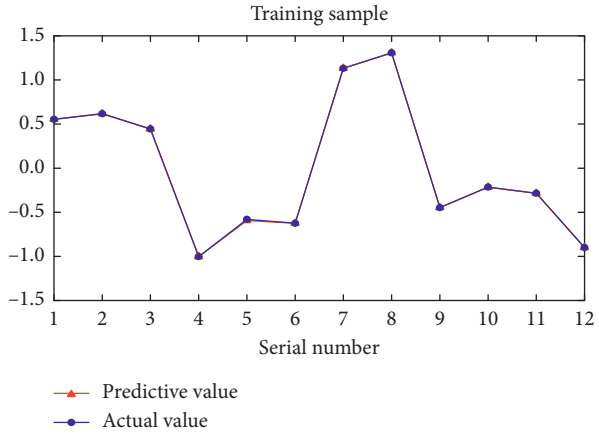

Figure 24: Residual training samples.

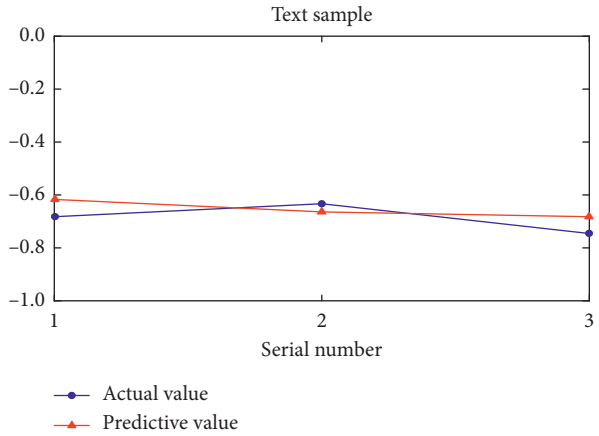

Figure 25: Residual test sample.

Table 14: Comparison of three models.

Period	Actual value	Predicted value		
		PSO-GM (1, 1)	PSO-BP	PSO-GM-BP
13	31.23	31.9099	31.1965	31.2924
14	31.92	32.5515	31.6132	31.8863
15	32.44	33.1876	32.1754	32.5039

Table 15: Comparison of relative error of three models.

Period	Relative error (%)		
	PSO-GM (1, 1)	PSO-BP	PSO-GM-BP
13	−2.18	0.11	−0.20
14	−1.98	0.96	0.10
15	−2.30	0.82	−0.20
Average relative error	2.15	0.63	0.17

data, using GM (1, 1) model and PSO-GM (1, 1) model, respectively, for prediction, PSO-GM (1, 1) model has improved the prediction accuracy of the two kinds of data, and Model stability is also better.

(3) The PSO optimization algorithm is selected to optimize the weight and threshold, and the PSO-BP network model was proposed. Combining the axial support force and inclinometer data obtained on site,

respectively, use the BP network and PSO-BP network to predict. PSO-BP network has significantly improved the prediction accuracy of the two kinds of data, and the convergence speed is faster.

7. Conclusion

(1) Combine the advantages and disadvantages of the PSO-GM (1, 1) model and the PSO-BP network to construct a PSO-GM-BP model. Through the comparative analysis of the prediction results of several models in this article, it could be concluded that the GM (1, 1) model and the BP neural network model can both predict more accurate results. With higher accuracy and more substantial applicability, the PSO-GM-BP model has the best predictive effect and can effectively guide the construction of foundation pit projects.

(2) The PSO algorithm is used to optimize the GM (1, 1) model and the BP network, which strengthens the accuracy and applicability of the model, but at the same time, there are some shortcomings and areas for improvement. While continuing to study, we will also consider a more in-depth comparison with other methods to find a more reasonable solution suitable for engineering intelligent applications.

Data Availability

The data used to support the findings of this study are available from the corresponding author upon request.

Conflicts of Interest

The authors declare that they have no conflicts of interest.

Acknowledgments

The authors would like to acknowledge the Fundamental Research Funds for the National Natural Science Foundation of China (No. 51474104) and Open Research Fund of Hunan Provincial Key Laboratory of Safe Mining Techniques of Coal Mines (No. E21835).

References

[1] J. D. Watson and F. H. C. Crick, "Molecular structure of nucleic acids: a structure for deoxyribose nucleic acid," *Nature*, vol. 171, no. 4356, pp. 737-738, 1953.

[2] S.-L. Shen, H.-N. Wu, Y. -J. Cui, and Z.-Y. Yin, "Long-term settlement behaviour of metro tunnels in the soft deposits of shanghai," *Tunnelling and Underground Space Technology*, vol. 40, pp. 309–323, 2014.

[3] Y. Tan and D. Wang, "Characteristics of a large-scale deep foundation pit excavated by the central-island technique in shanghai soft clay. I: bottom-up construction of the central cylindrical shaft," *Journal of Geotechnical and Geoenvironmental Engineering*, vol. 139, no. 11, pp. 1875–1893, 2013.

[4] Z.-J. Luo, Y.-Y. Zhang, and Y.-X. Wu, "Finite element numerical simulation of three-dimensional seepage control for deep foundation pit dewatering," *Journal of Hydrodynamics*, vol. 20, no. 5, pp. 596–602, 2008.

[5] S.-X. He, "Experimental researches on unloading deformation of clay in excavation of foundation pit," *Rock and Soil Mechanics-Wuhan-24.1: ISSU*, vol. 82, pp. 17–20, 2003.

[6] H.-F. Liu, "Study of a gray genetic BP neural network model in fault monitoring and a diagnosis system for dam safety," *ISPRS International Journal of Geo-Information*, vol. 7, no. 1, 4 pages, 2018.

[7] T. Feng, "Research of combination forecasting model based on improved analytic hierarchy process," *EURASIP Journal on Wireless Communications and Networking*, vol. 1, p. 182, 2018.

[8] C. Zhang, J.-Z. Li, and H. E. Yong, "Application of optimized grey discrete verhulst–BP neural network model in settlement prediction of foundation pit," *Environmental Earth Sciences*, vol. 78, no. 15, p. 441, 2019.

[9] W. Zhang, C. Wu, Y. Li, L. Wang, and P. Samui, "Assessment of pile drivability using random forest regression and multivariate adaptive regression splines," *Georisk: Assessment and Management of Risk for Engineered Systems and Geohazards*, vol. 10, pp. 1–14, 2019.

[10] Z. Ji, B. Wang, S. Deng, and Z. You, "Predicting dynamic deformation of retaining structure by LSSVR-based time series method," *Neurocomputing*, vol. 137, pp. 165–172, 2014.

[11] Y. Yao, J. M. Becker, M. R. Ford, and M. A. Merrifield, "Modeling wave processes over fringing reefs with an excavation pit," *Coastal Engineering*, vol. 109, pp. 9–19, 2016.

[12] J. Wang, "Areal subsidence under pumping well–curtain interaction in subway foundation pit dewatering: conceptual model and numerical simulations," *Environmental Earth Sciences*, vol. 75, no. 3, p. 198, 2016.

[13] H. Wu, Y. Dong, W. Shi et al., "An improved fractal prediction model for forecasting mine slope deformation using GM (1, 1)," *Structural Health Monitoring: An International Journal*, vol. 14, no. 5, pp. 502–512, 2015.

[14] W. Xingke and W. Juan, "Study of deformation prediction of foundation pit based on Optimized support vector machine and chaotic BP neural network," *Tunnel Construction*, vol. 37, no. 9, 1105 pages, 2017.

[15] J. Cao, "Time series forecast of foundation pit deformation based on BP neural network," *Applied Mechanics and Materials*, vol. 55, 61 page, 2014.

[16] X. Li, J. Kong, and C. Wang, "Application of combined model with optimum weight in prediction of landslide deformation," *Nature Reviews Disease*, vol. 02, pp. 53–57, 2008.

[17] W. Deng, J. Xu, H. Zhao, and Y. Song, "A novel gate resource allocation method using improved PSO-based QEA," *IEEE Transactions on Intelligent Transportation Systems*, vol. 24, no. 5, 9 pages, 2020.

[18] W. Deng, J. Xu, Y. Song, and H. Zhao, "Differential evolution algorithm with wavelet basis function and optimal mutation strategy for complex optimization problem," *Applied Soft Computing*, vol. 2020, Article ID 106724, 2020.

[19] W. Deng, H. Liu, J. Xu, H. Zhao, and Y. Song, "An improved quantum-inspired differential evolution algorithm for deep belief network," *IEEE Transactions on Instrumentation and Measurement*, vol. 69, no. 10, pp. 7319–7327, 2020.